Dynamic Behaviour of Flow Through Three Circular Cylinders in Staggered Arrangement with Three Disturbance Bodies Around the Upstream Cylinder

Banta Cut, Sutardi[*], Wawan Aries Widodo
Department of Mechanical Engineering,
Faculty of Industrial Technology and Systems Engineering,
Institut Teknologi Sepuluh Nopember, Jl. Arief Rahman Hakim,
Sukolilo, Surabaya 60111, INDONESIA
[*]sutardi@me.its.ac.id

ABSTRACT

Studies on flow through cylinders have been widely carried out, both experimentally and numerically. The purpose of those studies is to obtain information about flow phenomena around the cylinder arrangement, such as aerodynamic forces, vortex shedding, and vortex-induced vibration. This study aims to evaluate the flow characteristics that pass through three circular cylinders arranged in a stagger and reduce the drag force (C_D) by adding 3 disturbance bodies (DB) around the upstream cylinder. The longitudinal distance L/D varies from 1.5 to 4.0, while the transversal distance T/D is kept constant. Next, the diameter ratio d/D is set to 0.16. The diameter of cylinder 1, D=25 mm, and the diameter of the DB, d=4 mm. The DB is placed around cylinder 1 at three angle locations with a gap, δ=4 mm. The study is performed using Ansys fluent® 19.1 software in 2-D unsteady RANS with the transition k-kl-omega turbulence model. The flow Reynolds number based on D is $22x10^4$. The results showed that the L/D and the use of DB affect the cylinder drag coefficient (C_D). There is a C_D reduction for cylinder 1 up to 20% at L/D=3.0. For cylinders 2 and 3, the reduction in C_D occurred at L/D=4.0 up to approximately 13% and 17%, respectively.

Keywords: *Cylinder Arrangement; Disturbance Body; Transition K-Kl-Omega; Drag Coefficient*

Nomenclature

U	free stream velocity of the fluid (m/s)
V_{max}	maximum velocity of fluid (m/s)
D	diameter of the main cylinder (m)
d	diameter of disturbance body (m)
T/D	non-dimensional transversal distance
L/D	non-dimensional longitudinal distance
Re	Reynolds number
P/D	pitch ratio
G/D	non-dimensional distance of the gap between the main circular cylinder and the disturbance body
DB	disturbance body
θ	position angle of DB
VIV	vortex-induced vibration
ρ	the density of fluid (kg/m^3)
IDB	inlet disturbance body
FVM	finite volume method
Nu	Nusselt number
MRT	multiple relaxation time
δ	distance between cylinder 1 and DB (m)
WIV	wake-induced vibration
LBM	lattice Boltzmann method
μ	absolute viscosity of the fluid (Pa.s)
u$_i$, v$_j$	velocity component in the *i*th or *j*th direction (m/s)
t	time (s)
p	pressure (Pa)
C_D	drag coefficient $\qquad C_D = \dfrac{F_D}{{}^1\!/_2\,\rho V^2 A}$
$C_{D'}$	drag coefficient fluctuation
C_L	lift coefficient $\qquad C_L = \dfrac{F_L}{{}^1\!/_2\,\rho V^2 A}$
$C_{L'}$	lift coefficient fluctuation
t	time step (s)
Ri	Richardson number
St	Strouhal number
f	frequency (Hz)
PSD	power spectral density

Introduction

The use of circular cylinders in engineering with various configurations such as in-line, tandem, side-by-side, staggered, and square arrays, has been widely used. This application creates an interaction between the fluid flow and the bluff body arrangement resulting in drag and lift forces on the bluff body. Modifications to various configurations of the bluff body arrangement or constructions are intended to reduce drag force, thus reducing the overall load, and the constructions will last longer. Efforts to reduce the drag have inspired the authors to conduct further research on the flow passes through three circular cylinders in a staggered arrangement with *L/D* variations and the use of a Disturbance Body (DB).

The research on flow through a single-cylinder [1] shows that the interaction between the fluid flow and the bluff body is strongly influenced by the free-stream velocity, the specimen's shape, and the surface roughness. These variables will determine the magnitude of the drag force. The effect of the Reynolds number on the flow through a circular cylinder concluded that the greater the Reynolds number, the more turbulent the flow that results in the separation point being delayed [2]. Another study explains that turbulent flow can overcome the adverse pressure gradient effect and reduce wake area and drag [3]. The addition of DB in front of a single cylinder has also been investigated experimentally [4] as well as numerically [5]. The last two studies showed that there is drag reduction on the circular cylinder and the system.

Similar research shows that there is more significant influence of Reynolds number (*Re*) compared to the influence of *d/D* and *L/D* on the decrease in pressure drag [6]-[7]. Circular cylinders in tandem arrangement situated in a narrow channel with variations of *L/D* and *Re* also greatly affect the decrease in pressure and drag [8]. The use of two cylindrical DB in front of the upstream cylinder [9]-[11], is very effective in reducing the drag that occurs in the main circular cylinder. The fluid flow through two circular cylinders in various arrangements with variations of *Re* and *P/D* indicates that the flow characteristics are very similar to that of the flow through a single cylinder [12].

Flow through two circular cylinders in tandem and staggered arrangement, both elastically or permanently installed has been studied [13]-[14]. It shows that the downstream cylinder is affected by the presence of Wave-Induced Vibration (WIV), and the effect is very sensitive to differences in the distance (*L/D*). The study of two cylinders in staggered arrangement placed in a planar shear flow has also been studied [14]. Two different distances were used in that study, namely *P/D*=1.125 and 1.250, and were set at shear parameters *K* of 0.00 and 0.05. At a condition of no shear flow which is referred to as uniform flow, the flow behaviour around the two cylinders behaves as a single cylinder. Similar research [15]-[16], indicates that the peak of the vortex shedding is weaker and more swirling near the base of the

cylinder. At short and medium distances, there has been a change in the Strouhal number followed by a change in the flow pattern. Other research with similar methods has also been carried out, namely numerical simulation using the LES method. The result shows that the inner lift force occurs at a distance P/D=1.5 - 3.0 and angle=10° because the existence of the flow passes through the narrow gap between the cylinders [17]. The lift force on the outer side occurs at a distance of P/D=3 - 4 and angle=20°, due to the interaction between the vortices that are released from the upstream cylinder and re-attaches to the downstream cylinder. Experimental test of flow passing through two circular cylinders arranged side by side, tandem, and staggered has also been studied [18]. The result shows that at low flow velocity $U^* < 7$, the vibration can be damped, while at higher flow velocity $U^* \geq 7$, the oscillation increases. In addition, in the tandem arrangement, the vibration is smaller [18].

The flow passes through three circular cylinders [19]-[20] in an equilateral triangle arrangement, showing that the drag reduction for the upstream cylinder is found at an angle, α=10°. For the upper downstream cylinder, it occurs at an angle of 25°, and for the lower downstream cylinder, it occurs at an angle of α=20° [19]. The smallest drag coefficient occurs at distances (N/d)=1.7 and 2.2 [20]. The use of IDB in front of the upstream cylinder [21] with L/D variations can reduce the drag for the upstream cylinder and also significantly affects the distribution of Cp and the velocity profile behind three circular cylinders in a staggered arrangement. Similar studies have also been carried out using multiple relaxation time (MRT) based lattice Boltzmann method (LBM) [22]-[23]. The results of these studies show that the staggered arrangement has a significant effect on the wake structure, force fluctuations, and vortex shedding. Flow through three circular cylinders with varying turning angle β=0°, 30°, and 60° shows that the upstream cylinder greatly affects the downstream cylinder, and the drag coefficient decreases as the velocity decrease [24]. Yang et al. [25] showed that P/d and turning angle affect significantly the flow passes three equilateral circular cylinders arrangement. Simulation studies of the flow through three circular cylinders in tandem, side by side, and staggered arrangement using the Boltzmann boundary-lattice method indicate various flow patterns that influence the vortex shedding structures and flow properties [26]. The average shift position and hydrodynamic forces of two circular cylinders arranged side by side located behind a stationary upstream cylinder are significantly influenced by the upstream cylinder wake and the wake-vortex interaction of the upstream cylinder [27].

Numerical simulation using the 2-D finite volume method for three circular cylinders in a triangular arrangement has also been carried out [28]. The variations in L/D, the orientation angle (0° and 180°), and the flow Reynolds number (Re=100 and 200) were used in the study. At Re=100, the flow behind the downstream cylinder is monostable (similar to a single cylinder), while at Re=200, the bias flow phenomenon disappears. The study

shows that the combination effects of the flow Reynolds number and the distance *L/D* significantly influence the biased-flow pattern of the wake behind the cylinder arrangement. A study of flow through square cylinders in staggered arrangement [29] shows that the flow is periodic and organized and that there are flow disturbances over a large distance ratio. However, when the distance ratio decreases, the flow becomes more turbulent due to the influence of the larger flow disturbance. The same study with variations of Reynolds number and transversal distance (S_T/D) and longitudinal distance (S_L/D), shows that the ratio of distance and Re affect significantly the flow and wake formed behind the bluff body arrangement [30]-[31]. The effects of distance (S_T/D) and (S_L/D) on C_D and *Nu* change significantly with changes in the value of *Ri* [31].

Based on the previous studies, we performed a numerical simulation study of the flow through three circular cylinders in the staggered arrangement by adding three DB around the upstream cylinder. The staggered arrangement of the cylinders is set so that varying in longitudinal distance *L/D* and are constant in transversal distance *T/D*. This numerical simulation was performed using the k-kl-omega transition turbulence model and was analysed at $Re=2.2 \times 10^4$. The distribution of *Cp*, distribution of C_D, distribution of C_L, and Strouhal number are presented and analysed in this study.

Numerical Methods

Basic equations and numerical simulation domain
The basic equations, which include the continuity equation and the momentum equation, can be written as shown in Equation (1) and Equation (2), respectively:

$$\frac{\partial v_i}{\partial x_i} = 0 \tag{1}$$

$$\rho \frac{\partial v_i}{\partial t} + \rho v_j \frac{\partial v_i}{\partial x_j} + \frac{\partial P}{\partial x_i} - \mu \nabla^2 v_i = 0, \tag{2}$$

where v_i, ρ, t, μ, and *P* represent the components, namely velocity, density, time, absolute or dynamic fluid viscosity, and pressure, respectively. Figure 1 shows the numerical simulation domain for three circular cylinders arranged in a staggered configuration with three *DB*'s around cylinder 1.

The numerical simulation domain and the meshing model used are quadrilateral-submap, as shown in Figures 2(a) and (b). Several parameters in determining variation can be seen in Table 1.
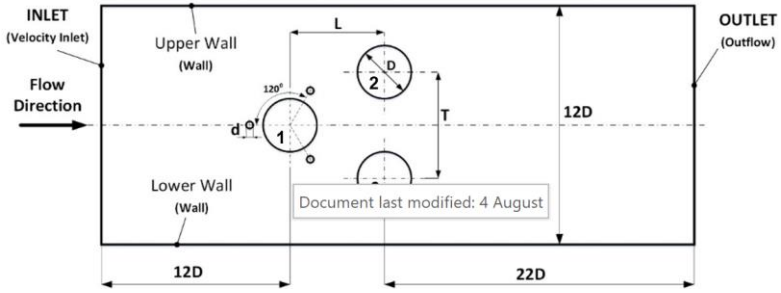
Figure 1: The numerical simulation domain and boundary conditions for
three circular cylinders in a staggered arrangement with three DB's

Meshing solution and determination of boundary conditions
Meshing is made using Gambit 2.4.6 software. The type of meshing in this
numerical simulation is a quadrilateral structured 2-D mesh, as shown in
Figure 2. The boundary conditions in this study are shown in Table 2.

(a)   (b)
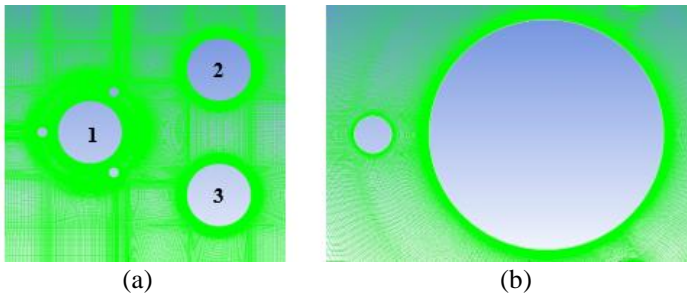
Figure 2: (a) Meshing of three circular cylinders in a staggered arrangement
with three DB around cylinder 1, and (b) meshing cylinder 1 with DB
(enlargement)

Table 1: Research parameters

Research parameters	
Reynolds number	2.2×10^4
The ratio of the distance between the centres of circular cylinders L/D and T/D	L/D=1.5, 2.0, 3.0, and 4.0 T/D=2.0
Ratio of the diameter of disturbance body to the circular cylinder, d/D	0.16
The ratio of the gap between the DB and the circular cylinder to the circular cylinder diameter, δ/D	0.16

Processing

Physical phenomenon modelling
This numerical simulation was carried out using ANSYS Fluent® software version 19.1, with the modelling of physical phenomena including pressure-based solver, unsteady flow, and the transition *k-kl-ω* turbulence model [32]-[33]. This turbulence model was chosen for the flow with *Re* in the transition range [32]-[33]. The fluid is air at atmospheric pressure with an average temperature of 27 °C. The air density (ρ) and the absolute fluid viscosity (μ) are set to be 1.225 kg/m^3 and 1,7894 x 10^{-5} kg/m.s, respectively.

Boundary conditions and solution method
In this study, the inlet velocity of the fluid is 14.1 m/s which corresponds with the flow with the Reynolds number of 2.2x10^4. The inlet turbulence intensity and the hydraulic diameter are to be set at 0.04 and 300 mm, respectively. The solution method for the pressure-velocity coupling is set as SIMPLEC, while the spatial discretization for pressure, momentum, turbulent kinetic energy, and the specific dissipation rate is set to be the second order upwind to obtain good accuracy on the simulation results. The residual value is set on the order of 10^{-6}, and the method used for initialization is the hybrid initialization method.

Table 2: Boundary conditions

Name	Type
Inlet	Velocity inlet
Outlet	Outflow
Upper wall	Wall
Lower wall	Wall
Circular cylinder	Wall
Disturbance body (DB)	Wall

To be able to capture the phenomenon of vortex shedding around and behind the bluff body arrangement, the iteration uses a small-time step size. The time step size value is based on the Strouhal number. For flow passes through a circular cylinder, the Strouhal number within a quite wide Reynolds number range is approximately 0.2 [34]. Then;

$$St = 0.2 = \frac{f \, x \, D}{U} \, . \tag{3}$$

Next, the time cycle and time step size are determined using Equation (4).

$$t = \frac{1}{f} \tag{4}$$

Post-processing

In the post-processing of the numerical simulation, a grid independence test is performed to evaluate the best meshing quality with the smallest error. The grid independence test is carried out using six types of meshing density, starting from a loose mesh (coarse), medium, fine, and very fine. The results of this test are then expressed in the form of Y^+ and drag coefficient (C_D) (Tables 3 and 4), and compared with the results of previous studies [20], [23]. This Y^+ result is very necessary to obtain the best meshing density with the smallest error, also to determine the shear stress near the wall more accurately, and thus the smallest errors C_D.

  The results of numerical simulations for six types of meshing show that mesh D with a meshing density of 180,765, the average in Y^+ is 2.159 (see Table 3). This result is close to the results of mesh E and F, which are more tightly packed. Hence, for the need for running time efficiency, mesh D is used for the rest of this study. Evaluation of C_D (Table 4) shows that the smallest error of the six types of meshing is also for the mesh density of 180,765.

Table 3: Grid independence to Y^+

Number	Nodes	Y^+ Maximum	Y^+ Minimum	Y^+ Average
Mesh A	42,362	6.793	0.199	3.291
Mesh B	98,157	5.721	0.074	4.395
Mesh C	160,530	5.276	0.085	4.876
Mesh D	180,765	4.120	0.112	2.159
Mesh E	200,216	4.119	0.111	2.158
Mesh F	220,227	3.612	0.111	1.912

Table 4: Grid independence test of drag coefficient

Experiment [20]	Cyl. 1	Cyl. 2	Cyl. 3	Simulation [23]	Cyl. 1	Cyl. 2	Cyl. 3
C_D	0.7	0.8	1.0	C_D	0.9	1.1	1.1

Present study (Num)	C_D	Difference		C_D	Difference		C_D	Different	
Nodes	Cyl. 1	[20]	[23]	Cyl. 2	[20]	[23]	Cyl. 3	[20]	[23]
42,362	0.920	24%	2%	1.133	29%	3%	1.194	16%	8%
98,157	0.956	27%	6%	1.198	33%	8%	1.127	11%	2%
160,530	0.940	26%	4%	1.065	25%	-3%	1.152	13%	5%
180,765	0.919	24%	2%	1.089	27%	-1%	1.115	10%	1%
200,216	0.935	25%	4%	1.287	38%	15%	1.265	21%	13%
220,227	0.954	27%	6%	1.209	34%	9%	1.233	19%	11%

Results and Discussion

The results of the present study will be presented in the form of the distribution of Cp, C_D, and C_L. In addition, the velocity profiles and flow visualization results will also be presented and analysed. The C_D will be validated with experimental data [20] and numerical simulation results [23].

Distribution of *Cp* for three circular cylinders in a staggered arrangement with three disturbance bodies

The Cp distribution for the staggered arrangement of three circular cylinders with DB is shown in Figure 3. On cylinder 1 for all distances (*L/D*=1.5, 2.0, 3.0, and 4.0), the average stagnation point occurs at θ=24º (Table 5). Based on the present numerical results, the average location of the stagnation points, or more accurately the re-attachment points, of cylinder 1 do not change significantly with the presence of DB. Aside from the flow separation points from the cylinder shifted slightly backward resulting in a narrowing of the wake area. Up to this stage, however, we have not yet discussed the shift of the temporal stagnation and separation points. Furthermore, the flow interacts with the bluff body of cylinder 1 and experiences acceleration because the flow passes through a narrow space (Figure 4). This acceleration causes a decrease in Cp drastically to values of -1.6, -0.75, and -1.65 for *L/D*=1.5, 2.0, and 3.0, respectively. For *L/D*=4.0, the Cp is minimum (Cp_{min}= -1.67). The values of Cp_{min} for cylinder 1 for all distances (*L/D*) are almost the same (within ~ 4%), except for *L/D*=1.5. At a distance of *L/D*=1.5, some researchers called it a close distance between the upstream cylinder and the downstream cylinder, which is known as the bistable effect (Figure 3(a)). The separated flow from cylinder 1 and its impingement on cylinders 2 and 3 will have a significant effect on the wake of cylinder 1. Hence, the presence of the disturbance body (DB) on the main cylinder along with the attendance of the downstream cylinders affects the asymmetrical flow at the upper and lower sides. (Figures 4(a) and 5(a))

For cylinder 2 and cylinder 3, the distribution of Cp is symmetric, where the distribution of Cp on the upper side of cylinder 2 is similar to the distribution of Cp on the lower side of cylinder 3, and vice versa. Next, the distribution of Cp on the lower side of cylinder 2 resembles the distribution of Cp on the upper side of cylinder 3. However, the distribution of Cp in cylinder 2 and cylinder 3 is very fluctuating, where the maximum Cp occurs at different angles. At *L/D*=2 the maximum Cp occurs at an angle=4º for cylinder 2 and an angle=353º for cylinder 3. For *L/D*=1.5 and 3.0, the maximum Cp for cylinder 2 occurs at θ=4º, and for cylinder 3 is at θ=356º with the maximum Cp being 1.0. At *L/D*=4, however, the maximum Cp occurs at θ=12º for cylinder 2 and at θ=348º for cylinder 3. Figure 5 provides a detailed description of the flow velocity through a staggered arrangement of three circular cylinders with DB.

The phenomenon of bubble separation after the flow hits DB for all distances (*L/D*), can be seen in Figure 4. The flow that passes through the

narrow gap between DB at an angle of 0º with cylinder 1 and behind DB at θ =120º and 240º, causes the flow more turbulent and reattaches to the surface of cylinder 1 (Figure 5). The use of 3 DB at angles=0º, 120º, and 240º is intended to agitate the boundary layer development on the cylinder wall and delay the boundary layer separation from the cylinder wall. Figures 4 and 5 show a qualitative description of the location of the boundary separation due to the addition of interfering bodies. In addition, in Figure 5, the positions of stagnation and separation points have also been marked and have been included in Table 5. In Table 6, we show a comparison of the CD between this study and that of Yan et al. [23].
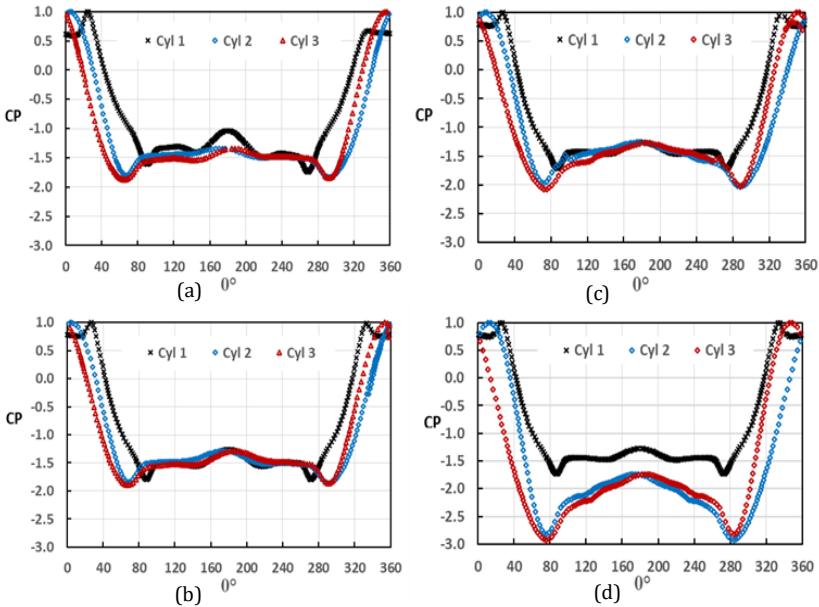
Figure 3: Distribution of *Cp* on three circular cylinders in staggered arrangement with three DB at angles of 0º; 120º, and 240º, (a) *L/D*=1.5, (b) *L/D*=2.0, (c) *L/D*=3.0, and (d) *L/D*=4.0

Vortex shedding formation behind the cylinder arrangement is also strongly influenced by the flow disturbances separated from the DB. For example, for *L/D*=2.0 and 3.0 with a certain time step, the vortex on the upper side rotates clockwise, while the vortex on the lower side rotates counterclockwise. The vortex movement above cylinder 2 and below cylinder 3 has high turbulence intensity. This vortex interaction is conjectured to be responsible for the highly fluctuating lift (C_L) of the cylinder.
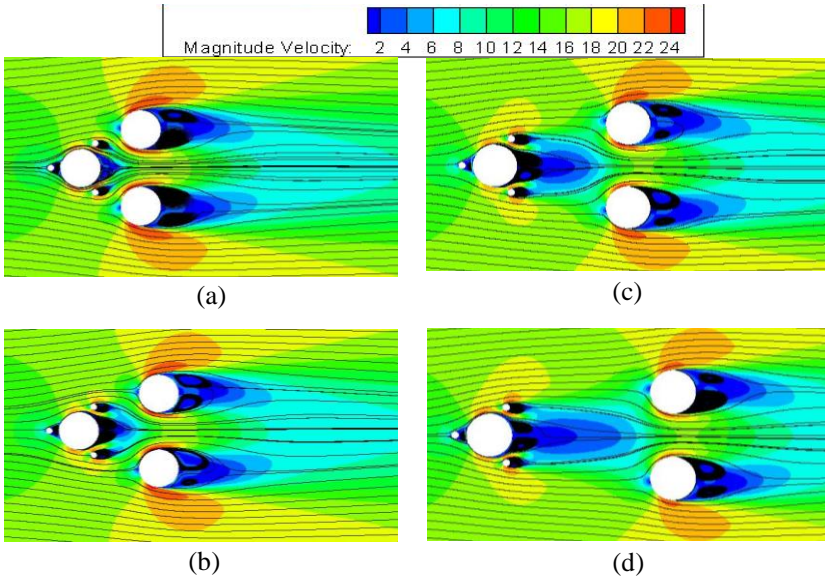
Figure 4: Visualization of velocity magnitude (m/s) on three circular cylinders in staggered arrangement with three DB at angles of 0º, 120º, and 240º; (a) *L/D*=1.5, (b) *L/D*=2.0, (c) *L/D*=3.0, and (d) *L/D*=4.0

Drag and lift coefficients

Figure 6 shows the distribution of $C_{D'}$ on all cylinders investigated in this study. The distribution of $C_{D'}$ of cylinder 1 for all values of *L/D*, is much smaller than the value of $C_{D'}$ of cylinders 2 and 3. This is because the use of DB around cylinder 1 has a significant effect on flow separation that occurs in cylinder 1. The separated flow from DB with high turbulence intensity interacts with the boundary layer on cylinder 1. The flow interaction results in the transition of the laminar boundary layer on cylinder 1 into the turbulent boundary layer. Therefore, this turbulent boundary layer can overcome the adverse pressure gradient effect on the cylinder surfaces and delay the boundary layer separation. This boundary layer separation delay causes the wake size behind the cylinder to become narrower resulting in $C_{D'}$ reduction on cylinder 1.

In general, the *L/D* has a significant effect on both $C_{D'}$ and $C_{L'}$ for all cylinders. As the distance increases, the character of C_D approaches as a single cylinder drags characteristics. On average, C_D on the cylinder 1 is lower than that of the C_D on cylinders 2 and 3. The low C_D on the first cylinder is probably due to the presence of the disturbance bodies. The C_D characteristics on cylinders 2 and 3 are almost similar since the positions of cylinders 2 and 3 relative to cylinder 1 are the same. The results of the present C_D compared with the previous experimental studies [20] are approximately within 6% and within approximately 6.5% with the numerical simulation results of [23].

(a)   (c)

(b)   (d)
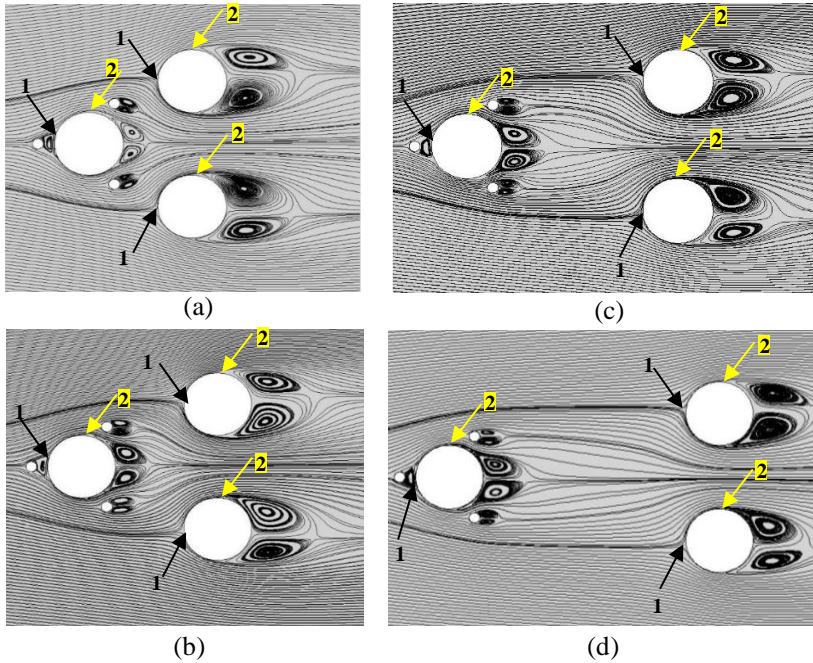
Figure 5: Velocity path line on three circular cylinders in staggered arrangement with 3 DB at angles of 0º, 120º, and 240º; (a) *L/D*=1.5, (b) *L/D*=2.0, (c) *L/D*=3.0, and (d) *L/D*=4.0; 1=stagnation point; 2=separation point

Table 5: Stagnation and separation point

	Position of stagnation and separation points (angle θ)					
	Cylinder 1		Cylinder 2		Cylinder 3	
L/D	Stagnation	Separation: up, low	Stagnation	Separation: up; low	Stagnation	Separation: up; low
1.5	24	93; 262	5	85; 276	354	84; 264
2	27	96; 264	4	93; 275	353	89; 261
3	27	96; 265	7	92; 268	350	95; 265
4	341	133; 259	12	95; 262	348	92; 265

Lift characteristics for all three cylinders are also significantly affected by the distance *L/D*. As the distance increases up to *L/D*=4.0, this lift fluctuation is still clearly discerned. Next, the separated flow from cylinder 1 followed by the nozzle effect of the flow in the gap between cylinders 2 and 3 may have a significant effect on the cylinder lift characteristics. The high flow

velocity between cylinders 2 and 3 creates a low-pressure region resulting in the unsymmetrical lift characteristics of the two cylinders.
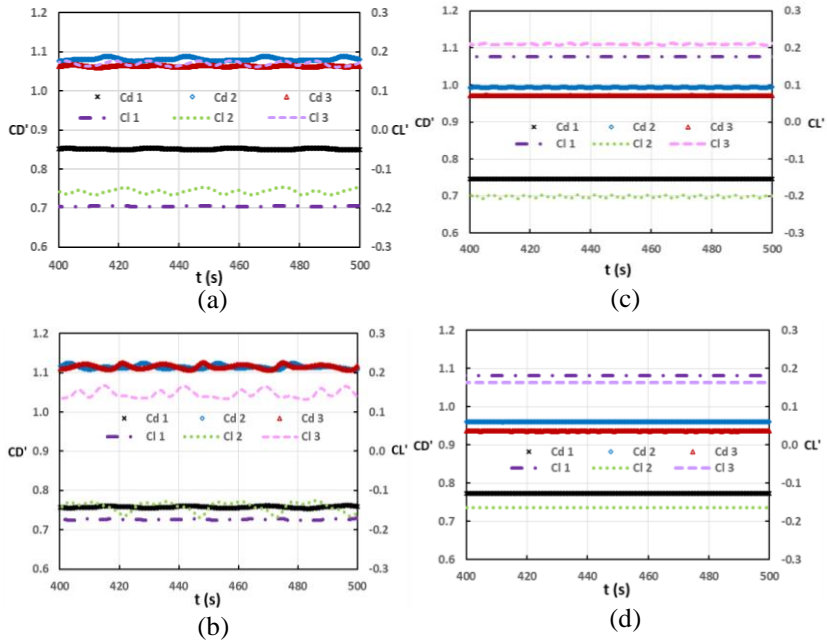
Figure 6: Coefficients of drag and lift on three circular cylinders in staggered arrangement with three DB at angles of 0º, 120º, and 240º; (a) *L/D*=1.5, (b) *L/D*=2.0, (c) *L/D*=3.0, and (d) *L/D*=4.0

Vorticity contour analysis

Figure 7 shows the vorticity magnitude of the three-cylinder arrangement with three DB around cylinder 1. The results show that the shear layer that is released from cylinder 1 for all *L/D* still greatly affects cylinder 2 and cylinder 3 events for the larger *L/D*. The vorticity development around those cylinders is strongly affected by the interaction of the two shear layers from the upper and lower sides of the cylinder arrangement. The larger the shear layer that is released, the greater the vorticity magnitude formed. In the flow with high shear, the vorticity magnitude is large, and the flow structure is very fluctuating between the upper and lower sides of the cylinder. This difference in vorticity can be seen in the different colours in Figure 7. The red colour shows the higher vorticity magnitude, while the blue indicates the lower value of vorticity or shear layer. This difference in vorticity region results in the different fluctuating C_L for different cylinder configurations. This vorticity is also strongly influenced by the Strouhal number ($St=fD/U$) that also affected by the ratio *L/D*.

Figure 8 shows power spectral density (PSD) based on the fluctuating C_L and the effect of L/D on the cylinder vibration frequency that is expressed in terms of Strouhal number (fD/U), where D and U are cylinder diameter and freestream velocity, respectively. The frequency, f, is adapted from the fluctuating lift signals for each cylinder. In the present study, as the distance L/D increases from 1.5 to 4.0, the amplitude of the fluctuating lift also increases. In general, the peak of the amplitude of the fluctuating lift of cylinder 1 is lower than that of cylinders 2 and 3, while the amplitudes of the fluctuating lift of cylinders 2 and 3 are almost similar. The Strouhal numbers in the present study are between 0.14 and 1.80, where these values are in good agreement with many literatures for the same Reynolds number range ($Re=2.2\text{x}10^4$) [35].
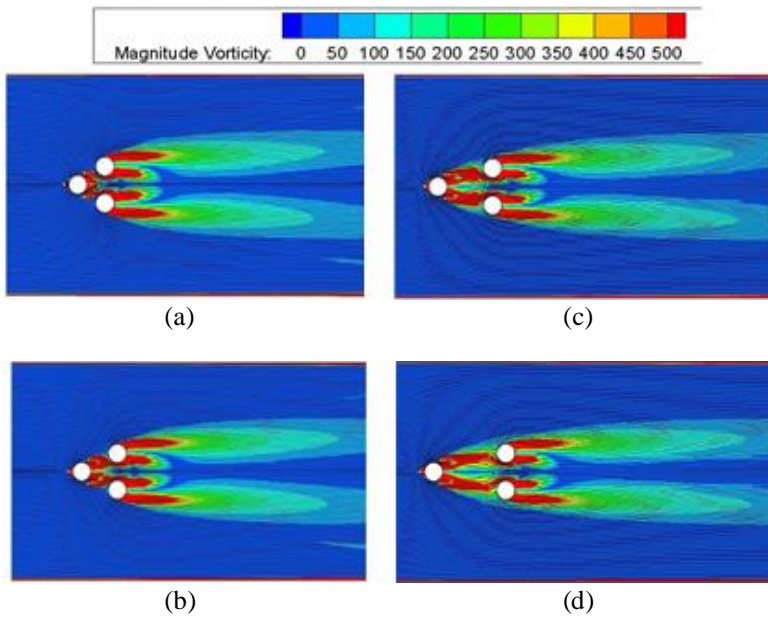
Figure 7: Contour of vorticity (s^{-1}) for three circular cylinders in staggered arrangement with three DB at angles 0º, 120º, and 240º; (a) L/D=1.5, (b) L/D=2.0, (c) L/D=3.0, and (d) L/D=4.0
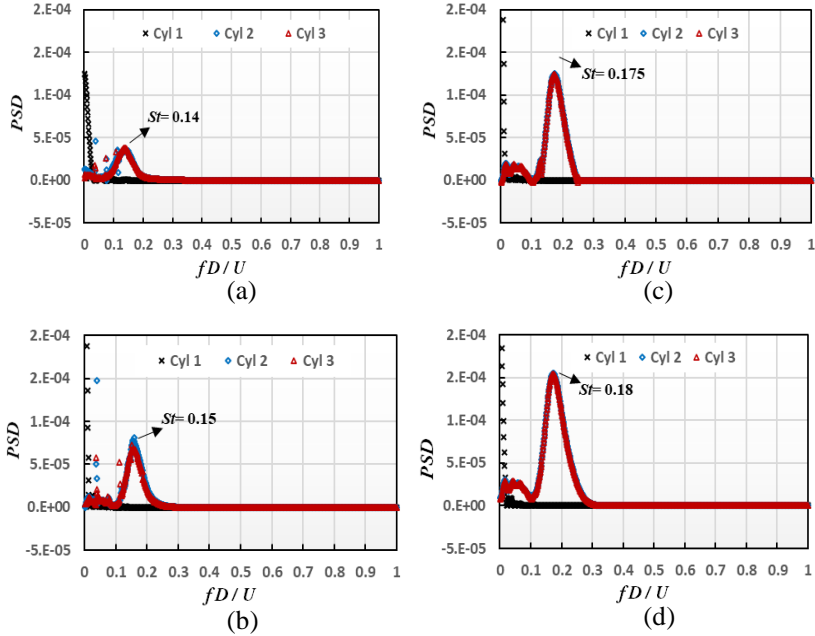
Figure 8: Strouhal number for three circular cylinders in staggered arrangement with three DB at angles 0º, 120º, and 240º; (a) *L/D*=1.5, (b) *L/D*=2.0, (c) *L/D*=3.0, and (d) *L/D*=4.0

Discussion

The distribution of $C_{D'}$ and $C_{L'}$ for three circular cylinders in staggered arrangement differs from that occurs in a single-cylinder configuration. The values of $C_{D'}$ and $C_{L'}$ for cylinder 1, cylinder 2, and cylinder 3 obtained in this study are in good agreement with the results of previous studies. The comparison of the present results and the previous experimental results [20] as well as the numerical simulation [23], are shown in Table 6 and Figure 9. However, the fluctuations in the distribution of $C_{D'}$ and $C_{L'}$ that occur in the simulation results of Yan et al. [23] are much larger. This is due to the difference in Reynolds number and the difference in the cylinders and the DB configuration between the present study and the previous ones.

The existence of three DB around cylinder 1 at positions of 0º, 120º, and 240º can reduce C_D as a whole system when compared with the C_D of Yan et al. study [23] (Table 6). The drag of cylinder 1 is reduced up to 6%, 18%, 20%, and 16% for *L/D*=1.5, 2.0, 3.0, and 4.0, respectively. For cylinders 2 and 3, the drag reductions are up to 2% and 3% at *L/D*=1.5, 11% and 13% at *L/D*=3,

and 14% and 17% at L/D=4. This C_D reduction is most probably due to the presence of the disturbance body (DB) situated around cylinder 1. The existence of this DB can significantly modify the boundary layer structure around cylinder 1 resulting in narrowing the wake size behind cylinder 1. This wake reduction causes a reduction in C_D, not only for cylinder 1 but also for cylinders 2 and 3. On the contrary, for L/D=2, there was an increase in C_D by 1% for cylinders 2 and 3. Furthermore, in this three-cylinder arrangement, cylinder 2 exhibits the lowest value of C_L among the others (Figure 9). The cause of low C_L for cylinder 2 is caused by the higher flow velocity passing through the narrow gap between cylinder 2 and cylinder 3.

Table 6: Comparison of C_D between the present study and Yan et al. [23]

Yan et al. [23]	Cylinder 1		Cylinder 2		Cylinder 3	
C_D	0.9		1.1		1.1	
Present Study	C_D		C_D		C_D	
L/D	Cylinder 1	Difference	Cylinder 2	Difference	Cylinder 3	Difference
1.5	0.852	-6%	1.080	-2%	1.063	-3%
2.0	0.761	-18%	1.115	1%	1.116	1%
3.0	0.748	-20%	0.995	-11%	0.974	-13%
4.0	0.776	-16%	0.962	-14%	0.940	-17%
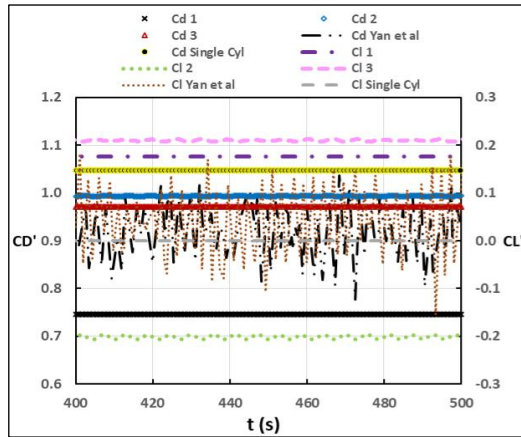
Figure 9: C_D and C_L for three circular cylinders in staggered arrangement with three DB at θ=0°, 120°, and 240° for L/D=3 compared with the previous studies [23]

Conclusion

Some conclusions that can be drawn from the results of the present study are as follows:

i. The use of three DB at θ=0º, 120º, and 240º, can reduce C_D significantly on three circular cylinders arranged in stagger. The maximum reduction in C_D is up to approximately 20% compared to the simulation results of Yan et al. [23]. The reduction in C_D seems a function of the longitudinal distance between cylinders (*L/D*).

ii. At *L/D*=1.5, C_D for the cylinder 2 is greater than that for cylinder 1, while at *L/D*=2.0 there was an increase in its C_D. With a further increase in *L/D*, the C_D for cylinder 2 tends to decrease.

iii. At *L/D*=1.5, there is a small reduction in C_D for cylinder 3, up to approximately 3%. At *L/D*=2.0, on the other hand, there is an increase in its C_D up to 1%, although this value is probably within the uncertainty value. Similar to that of C_D on cylinder 2, further increase in *L/D*, up to about 4.0, the C_D for cylinder 3 tends to decrease.

Contributions of Authors

The authors confirm the equal contribution in each part of this work. All authors reviewed and approved the final version of this work.

Funding

Conflict of Interests

All authors declare that they have no conflicts of interest.

Acknowledgment

References

[1] M. M. Zdravkovich, "Conceptual overview of laminar and turbulent flows past smooth and rough circular cylinders", *Journal of Wind Engineering and Industrial Aerodynamics*, vol. 33, no. 1–2, pp. 53–62, 1990. doi: 10.1016/0167-6105(90)90020-D.

[2] M. M. Zdravkovich, "The effects of interference between circular cylinders in cross flow† An earlier version as originally presented as an invited paper, entitled 'Forces on pipe clusters', at the International Symposium on Separated Flow around Marine Structures, Norwegian", *Journal of Fluids and Structures*, vol. 1, no. 2, pp. 239–261, 1987. doi: 10.1016/S0889-9746(87)90355-0.

[3] P. J. Pritchard and J. C. Leylegian, Fox and McDonald's Introduction To Fluid Mechanics, Eighth Edi. Manhattan: John Wiley & Sons, Inc, 2011.

[4] W. A. Widodo and P. Hariyanto, "Studi eksperimen pengaruh penambahan disturbance body terhadap karakteristik aliran resusun secara tandem dalam saluran sempit", *Jurnal Teknik ITS*, vol. 1, no. 1, pp. 122-125, 2012.

[5] P. F. Zhang, J. J. Wang, and L. X. Huang, "Numerical simulation of flow around cylinder with an upstream rod in tandem at low Reynolds numbers", *Applied Ocean Research,* vol. 28, no. 3, pp. 183–192, 2006. doi: 10.1016/j.apor.2006.08.003.

[6] A. M. Makka and W. A. Widodo, "Studi Eksperimen Aliran Melintasi Silinder Sirkular Tunggal Dengan Bodi Pengganggu Berbentuk Silinder Yang Tersusun Tandem Dalam Saluran Sempit Berpenampang Bujur Sangkar", *Jurnal Teknik ITS,* vol. 1, no. 1, pp. F92–F96, 2012.

[7] T. Tsutsui and T. Igarashi, "Drag reduction of a circular cylinder in an airstream", *Journal of Wind Engineering and Industrial Aerodynamics,* vol. 90, no. 1, pp. 527–541, 2002. doi: 10.1007/s10494-005-9008-0.

[8] A. Daloglu, "Pressure drop in a channel with cylinders in tandem arrangement", *International Communications in Heat and Mass Transfer,* vol. 35, no. 1, pp. 76–83, 2008. doi: 10.1016/j.icheatmasstransfer.2007.05.011.

[9] W. A. Widodo and N. Hidayat, "Experimental study of drag reduction on circular cylinder and reduction of pressure drop in narrow channels by using a cylinder disturbance body", *Applied Mechanics and Materials*, vol. 493, no. 5, pp. 198–203, 2014. doi: 10.4028/www.scientific.net/AMM.493.198.

[10] W. A. Widodo and R. P. Putra, "Reduction of drag force on a circular cylinder and pressure drop using a square cylinder as disturbance body in a narrow channel", *Applied Mechanics and Materials,* vol. 493, pp. 192–197, 2014. doi: 10.4028/www.scientific.net/AMM.493.192.

[11] A. A. A. Daman and W. A. Widodo, "Pengaruh Penambahan Inlet Disturbance Body Terhadap Karakteristik Aliran Melintasi Silinder

Sirkular Tersusun Tandem", *Thermofluid VI, Seminar Nasional Thermofluid VI Yogyakarta, 2014*, pp. 79–84, 2014.

[12] D. Sumner, "Two circular cylinders in cross-flow: A review", *Journal of Fluids and Structures,* vol. 26, no. 6, pp. 849–899, 2010. doi: 10.1016/j.jfluidstructs.2010.07.001.

[13] M. J. Janocha, M. C. Ong, P. R. Nystrøm, Z. Tu, G. Endal, and H. Stokholm, "Flow around two elastically-mounted cylinders with different diameters in tandem and staggered configurations in the subcritical Reynolds number regime", *Marine Structures*, vol. 76, pp. 1-20, 2021. doi: 10.1016/j.marstruc.2020.102893.

[14] H. Fukushima, T. Yagi, T. Shimoda, and K. Noguchi, "Wake-induced instabilities of parallel circular cylinders with tandem and staggered arrangements", *Journal of Wind Engineering and Industrial Aerodynamics*, vol. 215, p. 104697, 2021. doi: 10.1016/j.jweia.2021.104697.

[15] H. Li and D. Sumner, "Vortex shedding from two finite circular cylinders in a staggered configuration", *Journal of Fluids and Structures,* vol. 25, no. 3, pp. 479–505, 2009. doi: 10.1016/j.jfluidstructs.2008.11.001.

[16] W. Xu, H. Wu, K. Jia, and E. Wang, "Numerical investigation into the effect of spacing on the flow-induced vibrations of two tandem circular cylinders at subcritical Reynolds numbers", *Ocean Engineering*, vol. 236, p. 109521, 2021. doi: 10.1016/j.oceaneng.2021.109521.

[17] G. Wu, X. Du, and Y. Wang, "LES of flow around two staggered circular cylinders at a high subcritical Reynolds number of 1.4×10^5", *Journal of Wind Engineering and Industrial Aerodynamics*, vol. 196, no. 4, pp. 104044, 2020. doi: 10.1016/j.jweia.2019.104044.

[18] Q. Zou, L. Ding, R. Zou, H. Kong, H. Wang, and L. Zhang, "Two-degree-of-freedom flow-induced vibration of two circular cylinders with constraint for different arrangements", *Ocean Engineering*, vol. 225, p. 108806, 2021. doi: 10.1016/j.oceaneng.2021.108806.

[19] M. Tatsuno, H. Amamoto, and K. Ishi-i, "Effects of interference among three equidistantly arranged cylinders in a uniform flow", *Fluid Dynamics Research*, vol. 22, no. 5, pp. 297–315, 1998. doi: 10.1016/S0169-5983(97)00040-3.

[20] Z. Gu and T. Sun, "Classification of flow pattern on three circular cylinders in equilateral-triangular arrangements", *Journal of Wind Engineering and Industrial Aerodynamics*, vol. 89, no. 6, pp. 553–568, 2001. doi: 10.1016/S0167-6105(00)00091-X.

[21] B. Cut, R. Akram, Iskandar, A. Rahman, M. Zulfri, and Nazaruddin, "Experimental Review on Influence of Inlet Disturbance Body (IDB) at 30° Against Inhibitory Force Reduction on Three Circular Cylinders with Composed of Stagger (Variation L/D(constant=2), T/D = 1.5, 2, 3 & 4)", *IOP Conference Series: Materials Science and Engineering,* vol. 536, no. 1, pp. 1-9, 2019. doi: 10.1088/1757-899X/536/1/012017.

[22] S. Yang, W. Yan, J. Wu, C. Tu, and D. Luo, "Numerical investigation of vortex suppression regions for three staggered circular cylinders", *European Journal Mechanics - B/Fluids*, vol. 55, pp. 207–214, 2016. doi: 10.1016/j.euromechflu.2015.10.004.

[23] W. Yan, J. Wu, S. Yang, and Y. Wang, "Numerical investigation on characteristic flow regions for three staggered stationary circular cylinders," *European Journal of Mechanics - B/Fluids*, vol. 60, pp. 48–61, 2016. doi: 10.1016/j.euromechflu.2016.07.006.

[24] Y. Ma, Y. Luan, and W. Xu, "Hydrodynamic features of three equally spaced, long flexible cylinders undergoing flow-induced vibration", *European Journal of Mechanical - B/Fluids*, vol. 79, pp. 386–400, 2020. doi: 10.1016/j.euromechflu.2019.09.021.

[25] Z. Yang, X. Wang, J. H. Si, and Y. Li, "Flow around three circular cylinders in equilateral-triangular arrangement", *Ocean Engineering*, vol. 215, p. 107838, 2020. doi: 10.1016/j.oceaneng.2020.107838.

[26] R. Wang, Y. He, L. Chen, Y. Zhu, and Y. Wei, "Numerical simulations of flow around three cylinders using momentum exchange-based immersed boundary-lattice Boltzmann method", *Ocean Engineering*, vol. 247, p. 110706, 2022. doi: 10.1016/j.oceaneng.2022.110706.

[27] W. Chen, C. Ji, N. Srinil, Y. Yan, and Z. Zhang, "Effects of upstream wake on vortex-induced vibrations and wake patterns of side-by-side circular cylinders", *Marine Structures,* vol. 84, p. 103223, 2022. doi: 10.1016/j.marstruc.2022.103223.

[28] S. Zheng, W. Zhang, and X. Lv, "Numerical simulation of cross-flow around three equal diameter cylinders in an equilateral-triangular configuration at low Reynolds numbers", *Computer & Fluids* vol. 130, pp. 94-108, 2016. doi: 10.1016/j.compfluid.2016.02.013.

[29] D. Chatterjee and G. Biswas, "Dynamic behavior of flow around rows of square cylinders kept in staggered arrangement", *Journal of Wind Engineering and Industrial Aerodynamics*, vol. 136, pp. 1-11, 2015. doi: 10.1016/j.jweia.2014.10.019.

[30] Y. Gao, X. Qu, M. Zhao, and L. Wang, "Three-dimensional numerical simulation on flow past three circular cylinders in an equilateral-triangular arrangement", *Ocean Engineering*, vol. 189, p. 106375, 2019. doi: 10.1016/j.oceaneng.2019.106375.

[31] G. M. Barros, G. Lorenzini, L. A. Isoldi, L. A. O. Rocha, and E. D. dos Santos, "Influence of mixed convection laminar flows on the geometrical evaluation of a triangular arrangement of circular cylinders", *International Journal of Heat Mass Transfer*, vol. 114, pp. 1188-1200, 2017. doi: 10.1016/j.ijheatmasstransfer.2017.07.010.

[32] F. R. Menter, R. Langtry, S. Völker, and P. G. Huang, "Transition Modelling for General Purpose CFD Codes", *Flow Turbulence Combust*, vol. 77, pp. 31-48, 2005. doi: 10.1016/B978-008044544-1/50003-0.

[33] E. Salimipour, "A modification of the k-kL-ω turbulence model for

simulation of short and long separation", Computers & Fluids, vol. 181, pp. 67-76, 2019. doi: https://doi.org/10.1016/j.compfluid.2019.01.003.

[34] T. Camp and R. Figliola, "Fluid mechanics", in Mechanobiology Handbook, 2nd Ed., CRC Press, New York, pp. 23-44, 2011. doi: 10.2478/jtam-2013-0011.

[35] M. Mahbub Alam and Y. Zhou, "Strouhal numbers, forces, and flow structures around two tandem cylinders of different diameters", *Journal of Fluids and Structures*, vol. 24, no. 4, pp. 505-526, 2008. doi: 10.1016/j.jfluidstructs.2007.10.001.